PHYSICAL REVIEW A **79**, 063807 (2009)

Single-cycle pulse propagation in a cubic medium with delayed Raman response

Ajit Kumar* and Vimlesh Mishra
Department of Physics, Indian Institute of Technology, Hauz Khas, New Delhi 110016, India
(Received 16 January 2009; published 3 June 2009)

The propagation characteristics of a single-cycle pulse, at 0.8 μm wavelength, are studied numerically in one spatial dimension. It is shown that Raman term does influence the propagation characteristics by counteracting the self-steepening effect.

DOI: 10.1103/PhysRevA.79.063807 PACS number(s): 42.65.−k, 42.65.Tg, 42.65.Dr, 42.65.Sf

I. INTRODUCTION

During the last few years, remarkable developments have taken place in experimental techniques for generating and stabilizing ultrashort pulses [1–4] which led to the generation of high-intensity optical pulses with pulse duration equal to one period of the optical cycle or less. Such ultrashort pulses have found applications [5–10] in diverse areas of physics and technology including nonlinear optical devices, all-optical communication, medical diagnostics and imaging, controlled manipulation of chemical reactions and bond formation, and coherent quantum control of microscopic dynamics. As a result, presently, there is a great deal of interest in the study of propagation characteristics of a single- and a few-cycle pulses in linear as well as in nonlinear media.

In 1997, Brabec and Krausz [11] presented a novel model for nonlinear pulse propagation in the single-cycle regime, in which they showed that the concept of an envelope could be generalized for pulses with pulse duration equal to one optical period in terms of the invariance of the center frequency of the pulse under a phase shift of the electric field. Based on this, they derived a nonlinear pulse evolution equation that represents a generalization of the well-known nonlinear Schrodinger equation. This model equation has been successfully used by several authors [12–16] in various studies including nonlinear propagation dynamics of an ultrashort pulse in a hollow waveguide [12], supercontinuum generation by filamentation of a few-cycle pulse [13], estimation of the critical power for self-focusing in bulk media and in hollow waveguides [14], simulation of ultrabroadband light generation via self-channeling of few-cycle pulses in a noble gas [15], generation of ultrashort pulses in a hollow-core fiber filled with a noble gas [16], etc.

The main motivation of our work is to study the effect of the Raman term on the propagation characteristics of a single-cycle pulse. To the best of our knowledge, the influence of the Raman term on the propagation characteristics of a single-cycle pulse has not been considered earlier except in Ref. [17] where Chen and Lu have studied the effect of the Raman term on a 2.5 fs soliton pulse in a silica glass fiber. They have shown that for such short pulses the deviation from the soliton shape is very small. Other authors [18–21] have also taken the Raman term into account while studying the spatiotemporal dynamics (self-focusing) of optical pulses but for longer pulse durations. In the given paper we study the effect of the delayed nonlinear response on the propagation characteristics of a single-cycle pulse at 0.8 μm wavelength in a silica glass fiber within the slowly evolving wave approximation of Brabec and Krausz for a cubic medium. It is shown that the Raman term does influence the propagation characteristics of a single-cycle pulse by counteracting self-steepening and tending to restore the initial symmetric pulse shape. Our result is not only consistent with the results of Zozulya *et al.* [18], who studied the spatiotemporal self-focusing of a pulse with full width at half maximum (FWHM) of 90 fs but also explains why the deviation in the pulse in [17] is negligibly small for a 2.5 fs soliton pulse.

II. MODEL EQUATION

The nonlinear wave equation in a cubic nonlinear medium, including the delayed nonlinear response (Raman response), can be written as

$$\left(\vec{\nabla}_{\perp}^2 + \frac{\partial^2}{\partial z^2}\right)\vec{E}(\vec{r},t) = \frac{1}{c^2}\frac{\partial^2}{\partial t^2}\int_0^{\infty}\varepsilon(t')\vec{E}(\vec{r},t-t')dt' + \frac{\sigma\chi^{(3)}}{c^2}\frac{\partial^2}{\partial t^2}\{[\vec{E}(\vec{r},t)\cdot\vec{E}(\vec{r},t)]\vec{E}(\vec{r},t)\} + \left[\frac{(1-\sigma)\chi^{(3)}}{c^2}\right]\frac{\partial^2}{\partial t^2}\left\{\vec{E}(\vec{r},t)\int_0^{\infty}g_R(t') \times[\vec{E}(\vec{r},t-t')\cdot\vec{E}(\vec{r},t-t')]dt'\right\}, \quad (1)$$

where we have taken into account that the third-order nonlinear polarization consists of two terms:

$$\vec{p}_{nl} = \vec{p}_{nl}^{(1)} + \vec{p}_{nl}^{(2)} \equiv \sigma\varepsilon_0\chi^{(3)}[\vec{E}(\vec{r},t)\cdot\vec{E}(\vec{r},t)]\vec{E}(\vec{r},t) + \varepsilon_0\chi^{(3)}(1-\sigma)\vec{E}(\vec{r},t)\int_{-\infty}^{t}g_R(t-t')[\vec{E}(\vec{r},t')\cdot\vec{E}(\vec{r},t')]dt'. \quad (2)$$

Here, in the above equations, $\vec{E}(\vec{r},t)$ is the electric field vector, ε_0 is the permittivity of free space (vacuum), $\varepsilon(\vec{r},t)$ is the permittivity of the medium, $\chi^{(3)}$ is the third-order susceptibility, c is the speed of light in free space, σ is the fraction of the electronic contribution to nonlinear polarization, and $g_R(t)$ is the Raman response function. The value of σ is taken

*ajitk@physics.iitd.ac.in

to be 0.7 [22,23]. Under the assumption that only one vibrational mode, with linewidth $1/\tau_2$ and the eigenfrequency $1/\tau_1$, is important [24], the Raman response function is given by

$$g_R(t) = \frac{\tau_1^2+\tau_2^2}{\tau_1\tau_2^2} e^{-t/\tau_2} \sin\left(\frac{t}{\tau_1}\right), \tag{3}$$

where $\tau_1 = 12.2$ fs and $\tau_2 = 32$ fs. As shown by Brabec and Krausz [11], an envelope can be assigned to ultrashort pulses that contain at least one carrier cycle within their FWHM. Following that, we represent the electric field of a pulse, propagating in z direction, as

$$E(\vec{r},t) = A(\vec{r}_\perp,z,t)e^{i(\beta^{(0)}z-\omega_0 t)} + \text{c.c.}, \tag{4}$$

where $\vec{r}_\perp = x\hat{i}+y\hat{j}$, $A(\vec{r}_\perp,z,t)$, is the complex envelope amplitude, $\beta^{(0)}$ is the propagation constant and ω_0 is the carrier frequency. In what follows, we shall, for brevity, ignore the arguments of $A(\vec{r}_\perp,z,t)$ and write it simply as A unless it is necessary to write the arguments for clarity.

The Fourier transform of the first term on the right-hand side of Eq. (1) with respect to the time coordinate, Taylor expansion of $k(\omega)$ around the carrier frequency ω_0 followed by an inverse Fourier transform yields

$$\begin{aligned}
&[\vec{\nabla}_\perp^2 + \partial_z^2 + 2i\beta^{(0)}\partial_z - \beta^{(0)2}]A + [\beta^{(0)} + i\alpha_0/2 + i\beta^{(1)}\partial_t + \hat{D}]^2 A \\
&= -\frac{\sigma\omega_0^2\chi^{(3)}}{c^2}\left[A\left(1+\frac{i}{\omega_0}\partial_t\right)^2|A|^2 + |A|^2\left(1+\frac{i}{\omega_0}\partial_t\right)^2 A \right.\\
&\left. + |A|^2A\right] - \frac{(1-\sigma)\omega_0^2\chi^{(3)}}{c^2}\left(1+\frac{i}{\omega_0}\partial_t\right)^2 \\
&\times\left[A\int_0^\infty g_R(t')|A(t-t')|^2dt'\right],
\end{aligned} \tag{5}$$

where $\vec{\nabla}_\perp^2 = \partial^2/\partial x^2 + \partial^2/\partial y^2$ is the transverse Laplacian, $\partial_z = \partial/\partial z$, $\partial_t = \partial/\partial t$ and

$$\hat{D} = -\frac{\alpha_1}{2}\partial_t + \sum_{m=2}^{\infty}\frac{\beta^{(m)} + i\frac{\alpha^{(m)}}{2}}{m!}(i\partial_t)^m, \tag{6}$$

$$\beta^{(m)} = \text{Re}\left[\left(\frac{\partial^m k}{\partial\omega^m}\right)_{\omega=\omega_0}\right], \tag{7}$$

$$\alpha^{(m)} = 2\,\text{Im}\left[\left(\frac{\partial^m k}{\partial\omega^m}\right)_{\omega=\omega_0}\right] \tag{8}$$

is the dispersion operator. The quantities $\beta(\omega)$ and $\alpha(\omega)$ are the real and the imaginary parts, respectively, of $k(\omega)$. Taking into account that

$$\begin{aligned}
\left(1+\frac{i}{\omega_0}\frac{\partial}{\partial t}\right)^2|A|^2A &= A\left(1+\frac{i}{\omega_0}\frac{\partial}{\partial t}\right)^2|A|^2 + |A|^2\left(1+\frac{i}{\omega_0}\frac{\partial}{\partial t}\right)^2 A \\
&\quad + |A|^2A
\end{aligned} \tag{9}$$

and expanding $|A(t-t')|^2$ into a Taylor series around t', we obtain

$$\begin{aligned}
&[\vec{\nabla}_\perp^2 + \partial_z^2 + 2i\beta^{(0)}\partial_z - \beta^{(0)2}]A + [\beta^{(0)} + i\alpha_0/2 + i\beta^{(1)}\partial_t + \hat{D}]^2 A \\
&= -\frac{\sigma\omega_0^2\chi^{(3)}}{c^2}\left[\left(1+\frac{i}{\omega_0}\partial_t\right)^2|A|^2A\right] \\
&\quad - \frac{(1-\sigma)\omega_0^2\chi^{(3)}}{c^2}\left(1+\frac{i}{\omega_0}\partial_t\right)^2 \\
&\quad\times\left[|A|^2A\int_0^\infty g_R(t')dt' - A\frac{\partial|A|^2}{\partial t}\int_0^\infty t'g_R(t')dt'\right] \\
&= -\frac{\omega_0^2\chi^{(3)}}{c^2}\left[\left(1+\frac{i}{\omega_0}\partial_t\right)^2|A|^2A\right] \\
&\quad + \frac{(1-\sigma)\omega_0^2\chi^{(3)}}{c^2}T_R\left(1+\frac{i}{\omega_0}\partial_t\right)^2\left(A\frac{\partial|A|^2}{\partial t}\right).
\end{aligned} \tag{10}$$

We now go over to the moving frame by introducing the variables

$$\tau = t - \beta^{(1)}z = t - \frac{z}{v_g}, \quad \xi = z, \tag{11}$$

where v_g is the group velocity, divide Eq. (10) throughout by $2i\beta^{(0)}$ and take into account that $[\partial_\tau,\hat{D}]=0$ to get

$$\begin{aligned}
&\partial_\xi A - \frac{\beta^{(0)}}{2i}A + \frac{1}{2i\beta^{(0)}}\partial_\xi^2 A - \beta^{(1)}\partial_\tau A - \frac{\beta^{(1)}}{i\beta^{(0)}}\partial_{\xi\tau}^2 A + \frac{\beta^{(1)2}}{2i\beta^{(0)}}\partial_\tau^2 A \\
&+ \frac{1}{2i\beta^{(0)}}\vec{\nabla}_\perp^2 A + \frac{\beta^{(0)}}{2i}A - \frac{\alpha_0^2}{8i\beta^{(0)}}A + \frac{\alpha_0}{2}A - \frac{\beta^{(1)2}}{2i\beta^{(0)}}\partial_\tau^2 A \\
&+ \frac{\beta^{(1)}}{\beta^{(0)}}\partial_\tau(\hat{D}A) + \beta^{(1)}\partial_\tau A - i\hat{D}A - \frac{\alpha_0\beta^{(1)}}{2i\beta^{(0)}}\partial_\tau A + \frac{\alpha_0}{2\beta^{(0)}}\hat{D}A \\
&+ \frac{1}{2i\beta^{(0)}}\hat{D}^2A - \frac{\omega_0^2\chi^{(3)}}{2i\beta^{(0)}c^2}\left[\left(1+\frac{i}{\omega_0}\partial_\tau\right)^2|A|^2A\right] \\
&+ \frac{(1-\sigma)\omega_0^2\chi^{(3)}}{2i\beta^{(0)}c^2}T_R\left(1+\frac{i}{\omega_0}\partial_\tau\right)^2\left(A\frac{\partial|A|^2}{\partial\tau}\right) = 0.
\end{aligned} \tag{12}$$

Further simplification is made by adding and subtracting the expression

$$\frac{i}{\omega_0}\partial_\tau\left(\partial_\xi + \frac{\alpha_0}{2} - i\hat{D}\right)A \tag{13}$$

in Eq. (12). It yields

$$\begin{aligned}
&\left(1+\frac{i}{\omega_0}\partial_\tau\right)\left(\partial_\xi + \frac{\alpha_0}{2} - i\hat{D}\right)A \\
&\quad + \frac{4\beta^{(0)}n_2}{3in_0}\left(1+\frac{i}{\omega_0}\partial_\tau\right)^2|A|^2A + \frac{1}{2i\beta^{(0)}}\vec{\nabla}_\perp^2 A \\
&= i\left(\frac{\beta^{(0)}-\omega_0\beta^{(1)}}{\omega_0\beta^{(0)}}\right)\partial_\tau\left(\partial_\xi + \frac{\alpha_0}{2} - i\hat{D}\right)A \\
&\quad - \frac{1}{2i\beta^{(0)}}\left(\partial_\xi^2 - \frac{\alpha_0^2}{4} + i\alpha_0\hat{D} + \hat{D}^2\right)A \\
&\quad + \frac{4(1-\sigma)\beta^{(0)}n_2}{3in_0}T_R\left(1+\frac{i}{\omega_0}\partial_\tau\right)^2\left(A\frac{\partial|A|^2}{\partial\tau}\right).
\end{aligned} \tag{14}$$

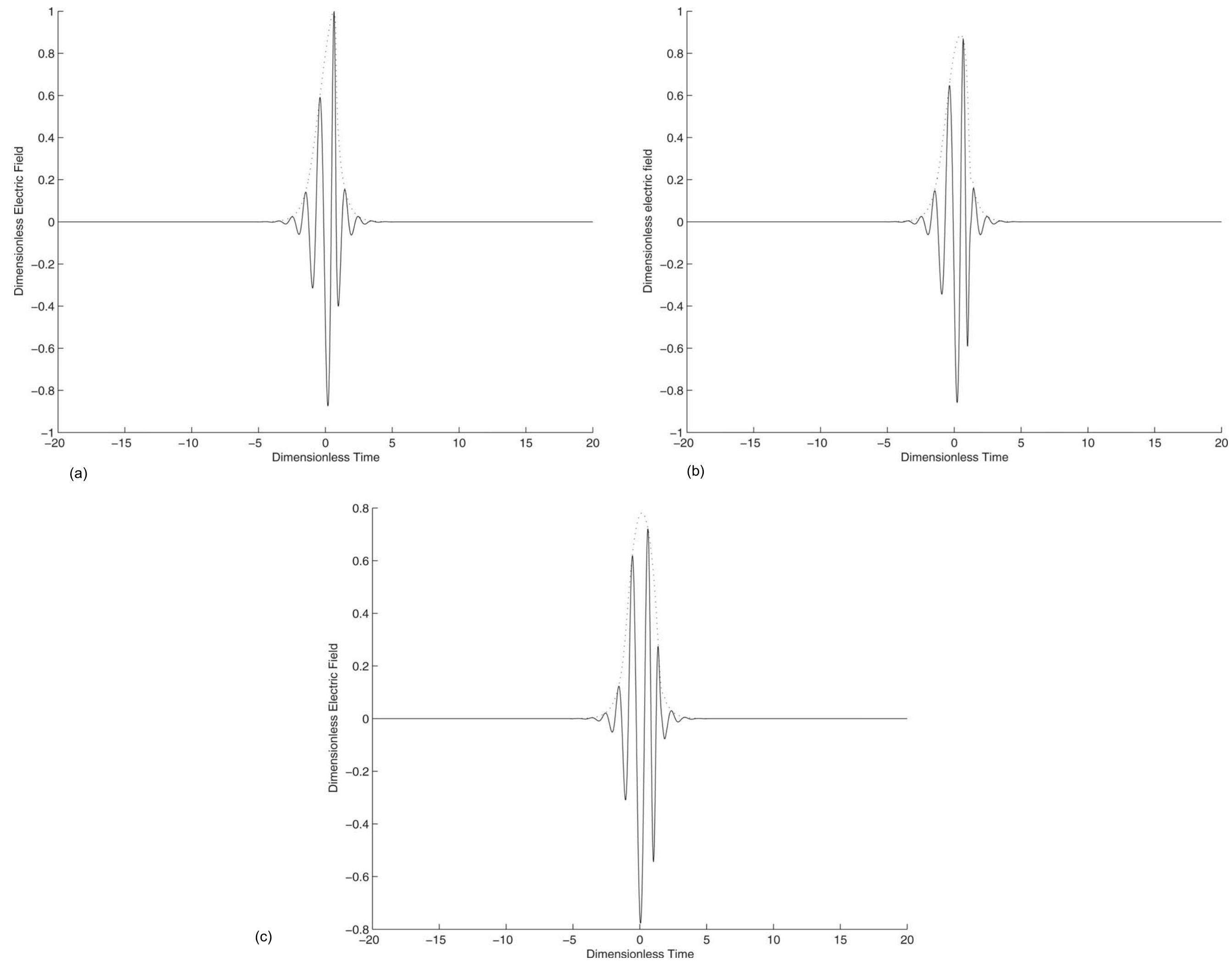

FIG. 1. (a) The dimensionless electric field $\bar{E}$ of a single-cycle pulse, at 0.8 μm wavelength, as a function of the dimensionless time $\bar{t}$, after 14.0 μm of propagation, for $n_2=3\times10^{-16}$ cm^2/W, $I=4\times10^{13}$ W/cm^2, $\beta^{(2)}=0$, and $\sigma=1.0$. The envelope is shown by the dotted curve. (b) The dimensionless electric field $\bar{E}$ of a single-cycle pulse, at 0.8 μm wavelength, as a function of the dimensionless time $\bar{t}$, after 14.0 μm of propagation, for $n_2=3\times10^{-16}$ cm^2/W, $I=4\times10^{13}$ W/cm^2, $\beta^{(2)}=0.039\,23$ fs^2/μm, and $\sigma=1.0$. The envelope is shown by the dotted curve. (c) The dimensionless electric field $\bar{E}$ of a single-cycle pulse, at 0.8 μm wavelength, as a function of the dimensionless time $\bar{t}$, after 14.0 μm of propagation, for $n_2=3\times10^{-16}$ cm^2/W, $I=4\times10^{13}$ W/cm^2, $\beta^{(2)}=0.039\,23$ fs^2/μm, $T_r=3$ fs, and $\sigma=0.7$. The envelope is shown by the dotted curve.

Note that in writing Eq. (14), we have made use of the expressions

$$\omega_0^2=\frac{\beta^{(0)2}c^2}{n_0^2},\quad \chi^{(3)}=\frac{8n_0n_2}{3},\quad \frac{\omega_0^2\chi^{(3)}}{2i\beta^{(0)}c^2}=\frac{4\beta^{(0)}n_2}{3in_0},\tag{15}$$

where n_0 and n_2 are the linear refractive index and the nonlinear Kerr coefficient, respectively.

Following Brabec and Krausz [11], we assume that the conditions

$$\left|\frac{\partial A}{\partial \xi}\right| \ll \beta^{(0)}|A|,\quad \left|\frac{\partial A}{\partial \tau}\right| \ll \omega_0|A|,\quad \left|\frac{\beta^{(0)}-\omega_0\beta^{(1)}}{\beta^{(0)}}\right| \ll 1,\tag{16}$$

representing the slowly varying wave approximation, hold good. The resulting equation is then

$$\left(1+\frac{i}{\omega_0}\partial_\tau\right)\left(\partial_\xi+\frac{\alpha_0}{2}-i\hat{D}\right)A+\frac{1}{2i\beta^{(0)}}\vec{\nabla}_\perp^2A + \frac{4\beta^{(0)}n_2}{3in_0}\left(1+\frac{i}{\omega_0}\partial_\tau\right)^2|A|^2A = \frac{4(1-\sigma)\beta^{(0)}n_2}{3in_0}T_R\left(1+\frac{i}{\omega_0}\partial_\tau\right)^2\left(A\frac{\partial|A|^2}{\partial\tau}\right).\tag{17}$$

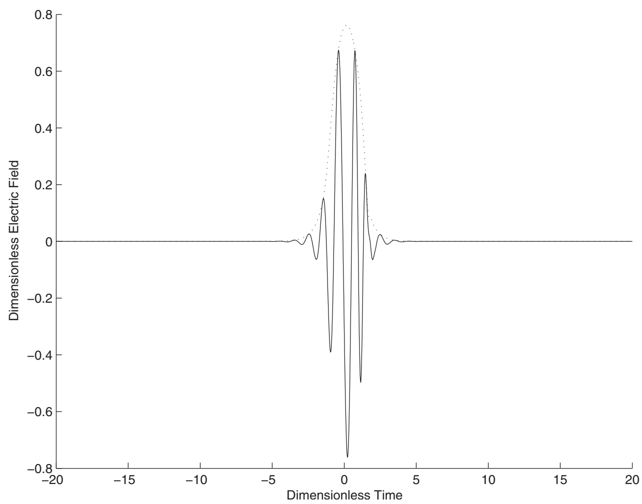

FIG. 2. The dimensionless electric field $\bar{E}$ of a single-cycle pulse, at 0.8 μm wavelength, as a function of the dimensionless time $\bar{t}$, after 16.3 μm of propagation, for $n_2=3\times10^{-16}$ cm^2/W, $I=4\times10^{13}$ W/cm^2, $\beta^{(2)}=0.039\,23$ fs$^2/\mu$m, $T_r=3$ fs, and $\sigma=0.7$. The envelope is shown by the dotted curve.

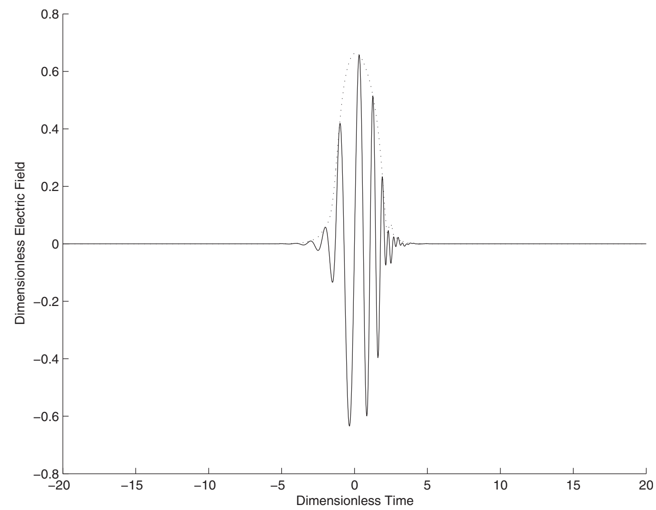

FIG. 3. The dimensionless electric field $\bar{E}$ of a single-cycle pulse, at 0.8 μm wavelength, as a function of the dimensionless time $\bar{t}$, after 32.6 μm of propagation, for $n_2=3\times10^{-16}$ cm^2/W, $I=4\times10^{13}$ W/cm^2, $\beta^{(2)}=0.039\,23$ fs$^2/\mu$m, $T_r=3$ fs, and $\sigma=0.7$. The envelope is shown by the dotted curve.

If we neglect damping and act on Eq. (17), from left, by the operator

$$\left(1+\frac{i}{\omega_0}\partial_\tau\right)^{-1} \quad (18)$$

we obtain

$$(\partial_\xi - i\hat{D})A + \frac{1}{2i\beta^{(0)}}\left(1+\frac{i}{\omega_0}\partial_\tau\right)^{-1}\vec{\nabla}_\perp^2 A + \frac{4\beta^{(0)}n_2}{3in_0}\left(1+\frac{i}{\omega_0}\partial_\tau\right)|A|^2A = \frac{4(1-\sigma)\beta^{(0)}n_2}{3in_0}T_R\left(1+\frac{i}{\omega_0}\partial_\tau\right)\left(A\frac{\partial|A|^2}{\partial\tau}\right). \quad (19)$$

If we confine ourselves to second-order dispersion alone, i.e., $\hat{D}=(-\beta^{(2)}/2)(\partial^2/\partial\tau^2)$ and multiply throughout by imaginary i, we get

$$i\frac{\partial A}{\partial\xi} - \frac{\beta^{(2)}}{2}\frac{\partial^2}{\partial\tau^2}A + \frac{1}{2\beta^{(0)}}\left(1+\frac{i}{\omega_0}\partial_\tau\right)^{-1}\vec{\nabla}_\perp^2 A + \frac{4\beta^{(0)}n_2}{3n_0}\left(1+\frac{i}{\omega_0}\partial_\tau\right)|A|^2A - \frac{4(1-\sigma)\beta^{(0)}n_2}{3n_0}T_R\left(1+\frac{i}{\omega_0}\partial_\tau\right)\left(A\frac{\partial|A|^2}{\partial\tau}\right)=0. \quad (20)$$

In the framework of slowly evolving wave approximation Eq. (21) governs the propagation characteristics of a single- and a few-cycle pulse in a cubic nonlinear medium with Raman response.

III. NUMERICAL RESULTS FOR ONE-DIMENSIONAL PROPAGATION

For pulse propagation in one spatial dimension, say, in a silica glass fiber, the above equation reduces to

$$i\frac{\partial A}{\partial\xi} - \frac{\beta^{(2)}}{2}\frac{\partial^2}{\partial\tau^2}A + \frac{4\beta^{(0)}n_2}{3n_0}\left(1+\frac{i}{\omega_0}\partial_\tau\right)|A|^2A - \frac{4(1-\sigma)\beta^{(0)}n_2}{3n_0}T_R\left(1+\frac{i}{\omega_0}\partial_\tau\right)\left(A\frac{\partial|A|^2}{\partial\tau}\right)=0. \quad (21)$$

In order to nondimensionalize the above equation, we introduce dimensionless quantities:

$$\bar{A}=\frac{A}{\sqrt{I}}, \quad \bar{\tau}=\frac{\tau}{\tau_p}, \quad \bar{z}=\frac{\xi}{L_D}, \quad (22)$$

where I is the input pulse intensity, τ_p is the pulse width and $L_D=T_0^2/|\beta^{(2)}|$ is the characteristics dispersion length. The dimensionless pulse evolution equation, for one-dimensional propagation, then reads

$$i\frac{\partial\bar{A}}{\partial\bar{z}} - \frac{\beta^{(2)}L_D}{2\tau_p^2}\frac{\partial^2\bar{A}}{\partial\bar{\tau}^2} + \frac{4\beta^{(0)}n_2IL_D}{3n_0}\left(1+\frac{i}{\omega_0\tau_p}\partial_{\bar{\tau}}\right)|\bar{A}|^2\bar{A} - \frac{4(1-\sigma)\beta^{(0)}n_2IL_D}{3n_0\tau_p}T_R\left(1+\frac{i}{\omega_0\tau_p}\partial_{\bar{\tau}}\right)\left(\bar{A}\frac{\partial|\bar{A}|^2}{\partial_{\bar{\tau}}}\right)=0. \quad (23)$$

We have numerically solved this equation, using split-step fast Fourier transform algorithm, for a single-cycle pulse at 0.8 μm wavelength. For pin-pointing the changes brought about by the Raman intrapulse scattering, in the propagation characteristics of a single- and a few-cycle pulse, we have considered three different cases: (i) propagation without dispersion and Raman effect, (ii) propagation including disper-

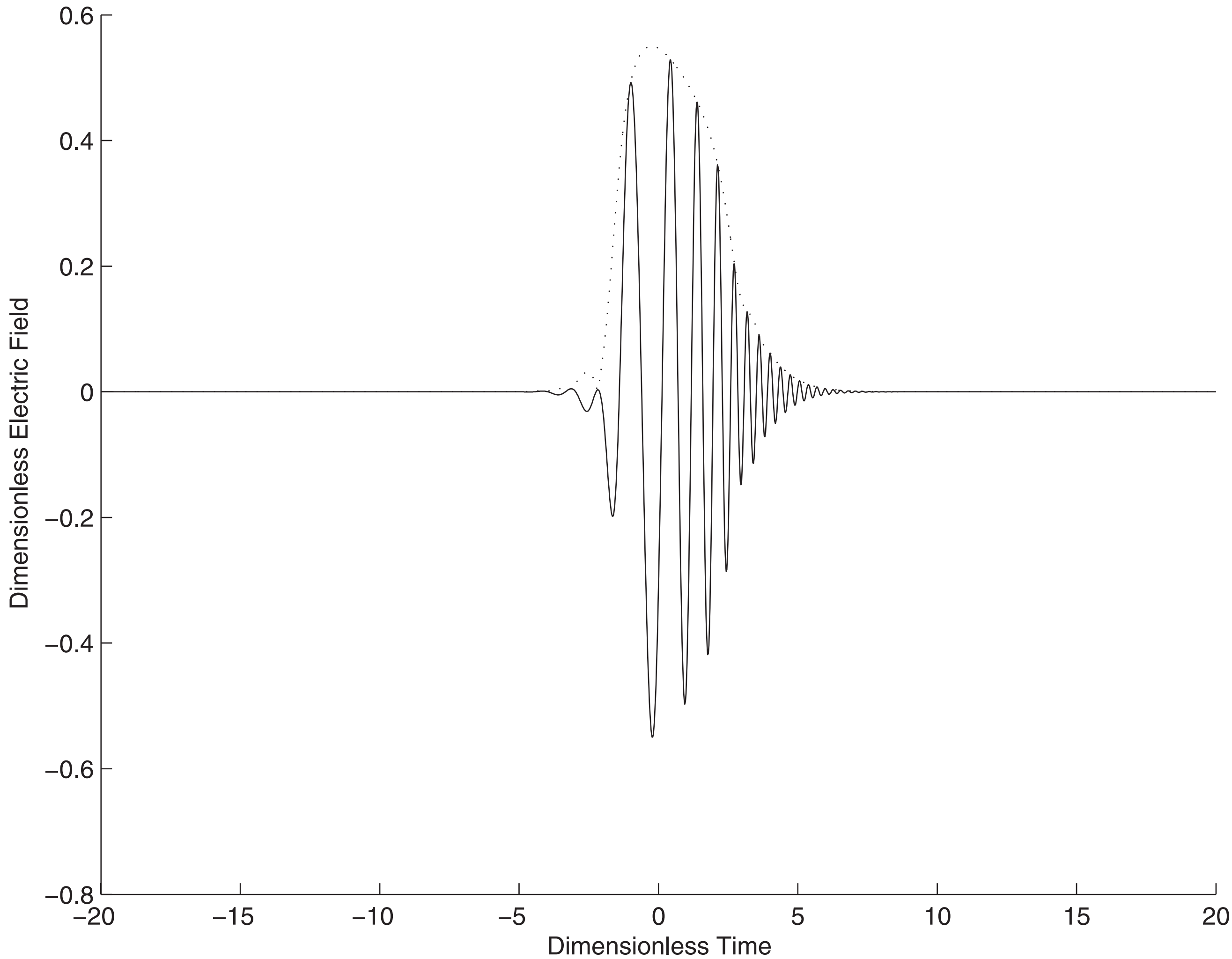

FIG. 4. The dimensionless electric field $\bar{E}$ of a single-cycle pulse, at 0.8 μm wavelength, as a function of the dimensionless time $\bar{t}$, after 65.2 μm of propagation, for $n_2=3\times10^{-16}$ cm^2/W, $I=4\times10^{13}$ W/cm^2, $\beta^{(2)}=0.039\,23$ fs$^2/\mu$m, $T_r=3$ fs, and $\sigma=0.7$. The envelope is shown by the dotted curve.

sive effects but ignoring Raman effect, and (iii) propagation with dispersion and Raman effect.

The input pulse is taken to be of hyperbolic secant form with:

$$A=\text{sech}(\tau/\tau_p). \tag{24}$$

The calculations have been carried out with the following parameters: $n_0=1.45$, $n_2=3\times10^{-16}$ cm^2/W, $I=4\times10^{13}$ W/cm^2, $\omega_0=2.3483\times10^{15}$ rad/sec, the speed of light $c=2.9979\times10^8$ m/sec, dispersion parameter $\beta^{(2)}=0.03923$ fs$^2/\mu$m [25], Raman response time $T_R=3$ fs, $\sigma=0.7$, and $\tau_p=2.67$ fs which corresponds to a single optical cycle at 0.8 μm wavelength.

In Figs. 1(a)–1(c) we have the dimensionless electric field, $\bar{E}(\bar{t})$, of a single-cycle pulse as a function of the dimensionless time $\bar{t}$ for propagation without dispersion and Raman term, with dispersion but without Raman response, and with both dispersion and Raman response, respectively. The plots are for 14 μm of propagation distance which is very close to the characteristic distance of self-steepening $z_s \equiv 14.45$ μm. As we see in Fig. 1(a) the pulse has undergone considerable self-steepening, as expected, with the center of the pulse shifted toward the trailing edge. Figure 1(b) shows that dispersion partially compensates for steepening of the wave front, however, as we see, the pulse is still dominated by self-steepening. In Fig. 1(c) the effect of the delayed Raman response, in helping the pulse to tend to regain its initial symmetric shape, is clearly visible. This can be physically understood as follows. In the frequency domain, self-steepening effect leads to a frequency shift toward the higher frequencies, in the trailing edge and toward the lower frequencies in the leading edge [26]. Since dispersion is positive, the leading edge moves faster than the trailing edge and imparts an asymmetry to the pulse by steepening the trailing edge. On the other hand, the frequency shift due to Raman effect is negative [24], i.e., toward the lower frequencies. Hence, the frequency shift due to self-steepening is counteracted by the frequency shift caused by the intrapulse Raman scattering. As a result the asymmetry of the pulse, introduced by self-steepening, gets neutralized and the symmetry of the pulse shape is restored.

In Fig. 2 we have the same plot but after a propagation distance of 16.3 μm. As we see, in Fig. 2, the pulse has broadened due to dispersion but the pulse shape continues to retain its symmetry even after the pulse has gone past the characteristic self-steepening length. However, for longer propagation distance dispersive effects start dominating leading to the generation of oscillatory structure in the trailing edge of the pulse. As the pulse travels further and further away from the characteristic self-steepening length more and more oscillatory structures are generated. This can be seen in Fig. 3 and Fig. 4 where we have the plots of the dimensionless electric field after 32.6 and 65.2 μm propagation distance, respectively.

IV. CONCLUSION

We have studied the influence of intrapulse Raman effect on the propagation characteristics of a single-cycle pulse in the framework of slowly evolving wave approximation. Our study shows that the Raman term counteracts the self-steepening effect by neutralizing the asymmetry caused by it and helps the pulse regain its initial symmetric temporal profile. Our result is not only consistent with the results of Zozulya *et al.* [18], who studied the spatiotemporal self-focusing of a pulse with FWHM of 90 fs, but also explains why the deviation in the pulse in Ref. [17] is negligibly small for a 2.5 fs soliton pulse. Further, we have shown that for propagation distances much larger than the characteristic self-steepening length, dispersion dominates pulse dynamics and generates dense oscillatory structure in the trailing edge of the pulse.

ACKNOWLEDGMENTS

We thank the referee for his valuable comments and suggested references which enabled us to put our results in right perspective compared to other results in the literature. V.M. thanks University Grants Commission, Government of India, for financial support.

[1] E. Goulielmakis, M. Uiberacker, R. Kienberger, A. Baltuska, V. Yakovlev, A. Scrinzi, Th. Westerwalbesloh, U. Kleineberg, U. Heinzmann, M. Drescher, and F. Krausz, Science **305**, 1267 (2004).
[2] R. López-Martens, K. Varjú, P. Johnsson, J. Mauritsson, Y. Mairesse, P. Salières, M. B. Gaarde, K. J. Schafer, A. Persson, S. Svanberg, C. G. Wahlström, and A. L'Huillier, Phys. Rev. Lett. **94**, 033001 (2005).
[3] G. D. Tsakiris, K. Eidmann, J. Meyer-ter-Vehn, and F. Krausz, New J. Phys. **8**, 19 (2006).
[4] M. B. Johnston, D. M. Whittaker, A. Dowd, A. G. Davies, E. H. Linfield, X. Li, and D. A. Ritchie, Opt. Lett. **27**, 1935 (2002).
[5] A. Scrinzi, M. Yu. Ivanov, R. Kienberger, and D. M. Villeneuve, J. Phys. B **39**, R1 (2004).
[6] M. Drescher and F. Krausz, J. Phys. B **38**, S727 (2005).
[7] T. Brabec and F. Krausz, Rev. Mod. Phys. **72**, 545 (2000).
[8] T. Misgeld and M. Kerschensteiner, Nat. Rev. Neurosci. **7**, 449 (2006).
[9] A. Baltuška Caronka, Th. Udem, M. Uiberacker, M. Hentschel, E. Goulielmakis, Ch. Gohle, R. Holzwarth, V. S. Yakovlev, A. Scrinzi, T. W. Hänsch, and F. Krausz, Nature (London) **421**, 611 (2003).
[10] P. Corkum, Nature (London) **403**, 845 (2000).
[11] T. Brabec and F. Krausz, Phys. Rev. Lett. **78**, 3282 (1997).
[12] D. Homoelle and Alexander L. Gaeta, Opt. Lett. **25**, 761 (2000).
[13] S. A. Trushin, K. Kosma, W. Fu, and W. E. Schmidt, Opt. Lett. **32**, 2432 (2007).
[14] G. Fibich and A. L. Gaeta, Opt. Lett. **25**, 335 (2000).
[15] E. Goulielmakis, S. Koehler, B. Reiter, M. Schultze, A. J. Verhoef, E. E. Serebryannikov, A. M. Zheltikov, and F. Krausz, Opt. Lett. **33**, 1407 (2008).
[16] M. Nurhuda, A. Suda, M. Hatayama, K. Nagasaka, and K. Midorikawa, Phys. Rev. A **66**, 023811 (2002).
[17] Chi-Feng Chen and Boren Lu, Optik (Stuttgart) **118**, 1 (2006).
[18] A. A. Zozulya, S. A. Diddams, and T. S. Clement, Phys. Rev. A **58**, 3303 (1998).
[19] G. Genty, P. Kinsler, B. Kibler, and J. M. Dudley, Opt. Express **15**, 5382 (2007).
[20] J. C. A. Tyrrell, P. Kinsler, and G. H. C. New, J. Mod. Opt. **52**, 973 (2005).
[21] V. G. Bespalov, S. A. Kozlov, Y. A. Shpolyansky, and I. A. Walmsley, Phys. Rev. A **66**, 013811 (2002).
[22] K. J. Blow and D. Wood, IEEE J. Quantum Electron. **25**, 2665 (1989).
[23] J. H. B. Nijhoft, H. A. Ferverda, and B. J. Hoenders, Pure Appl. Opt. **4**, 199 (1995).
[24] G. P. Agrawal, *Nonlinear Fiber Optics* (Academic, Boston, 1995).
[25] S. Diddams and Jean-Claude Diels, J. Opt. Soc. Am. B **13**, 1120 (1996).
[26] T. K. Gustafson, J. P. Taran, H. A. Haus, J. R. Lifshitz, and P. L. Kelley, Phys. Rev. **177**, 306 (1969).